ePproceedings Chemistry 2 (2016) 72-78

eISSN 2550-1453 http://eproceedings.chemistry.utm.my/

Characterizationof benzene-1,3,5-tricarboxamide organogel-gold nanoparticles composite

Aervina Binti Misron, Mustaffa Shamsuddin, and Hendrik Oktendy Lintang

Department of Chemistry, Faculty of Science, Universiti Teknologi Malaysia, 81310 Johor Bahru, Malaysia
Corresponding Author: mustaffa@kimia.fs.utm.my

Article history :
Received November 2016
Accepted December 2016

GRAPHICAL ABSTRACT

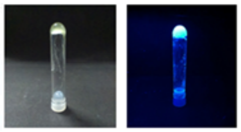

(a) Inverted test flow of **BTA$_{1+2}$** organogel and (b) **BTA$_{1+2}$** organogel observed under hand-held UV lamp 365 nm

ABSTRACT

Nanoparticles with particle size less than 10 nm have attracted much attention due to their unique properties in the field of optoelectronics, photovoltaics and catalysis. Gold nanoparticles (AuNPs) are well-known for its wide range of applications. However, AuNPs tends to agglomerate to form bigger cluster which limit its potential applications. Meanwhile, benzene-1,3,5-tricarboxamide (BTA) has been recognized as a simple and versatile organic motive for the formation of organogel by supramolecular self-assembly. Therefore, this study reports on the preparation of well-ordered AuNPs-organogel by doping Au into the co-assembled BTAs organogel. Firstly, a new organogel with 3-D networks having rectangular arrangement was prepared by mixing the BTA$_{C12}$ with BTA$_{C10TEG}$ with a molar ratio of 1:1. The as-synthesised BTAs organogel was then doped with 1%, 3% and 5% weight percent of 5 nm AuNPs to give AuNPs-organogel composite. The physico-chemical properties of the AuNPs-organogels were characterized by UV-Vis and Fluorescence spectroscopies, FT-IR and TEM analysis. Based on TEM analytical data, the organogel with 1% doped AuNPs give a well-ordered and homogenously distributed AuNPs morphology as compared with the 3% and 5% doped AuNPs. On the other hand, the photophysical studies of the AuNPs-organogel revealed that as the concentration of AuNPs increased, there was quenching in the fluorescence emission and SPR intensity. The photophysical studies suggested that an increase in the loading of AuNPs strongly affected the molecular arrangements of the co-assembled BTAs organogel.

Keywords: Gold nanoparticles, benzene-1,3,5-tricarboxamide, supramolecular self-assembly, organogel, physico-chemical properties.

1. INTRODUCTION

Nanotechnology is a new branch of nanosciences that helps to improve human lifestyles, revolutionize many industries, and development of new technology sectors such as catalysis and biological sensing [1, 2]. AuNPs are one of the main research subjects in nanosciences due to their unique optical, and catalytic potentials [3]. For example, AuNPs with unique optical properties are useful as biosensors in living whole cells especially in cancer diagnostics for medicinal application [4].

Noteworthy, there are many conventional methods in synthesizing AuNPs such as photo-reduction, thermal hydrogen reduction [5], electrochemical reduction, chloride reduction, and chemical vapor deposition [6]. However, most of these synthesizing methods often suffer from heavy agglomeration and inhomogeneity that further disrupted their well-defined size and shape. Hence, organogels have been used as a method for encapsulating nanomaterials with good spatial organisation and stability to overcome these issues.

Benzene-1,3,5-tricarboxamide (BTA) [7] is one of the example of organogel with chemical structure shows in Figure 1. Specifically, BTAs have been recognized to form organogelator by solvent entrapments in its SAFINs. Therefore, this project will focus on BTAs as soft-motive for organogelators due to its stability [7] and multiple supramolecular interactions as well as their solvent compatibility to be use for preparation of AuNPs –organogel by AuNPs doping.

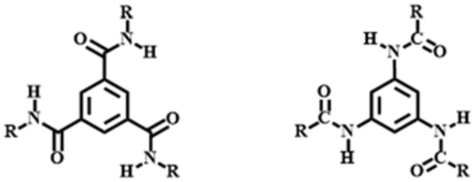

R = Alkyl, aryl, pyridyl, bipyridyl, porphyrinyl, triphenylyl, amino acid, dipeptide and benzo crown ethers.

Figure 1 General chemical structures of C=O and N-centered BTAs

This research will emphasize on synthesizing and characterizing BTAs organogel and BTAs organogel doped AuNPs of varied wt% forming AuNPs-organogel composites. In this case, BTAs organogel was doped with 1 wt%, 3 wt%, and 5 wt% AuNPs to study their physico-chemical properties. Resulting BTAs organogel showed different optical responses as compared to doped AuNPs-organogel. The composition of AuNPs be an important parameter in indicating the morphology and assembly of the AuNPs in BTAs organogel template. Good distribution, wel-ordered assembly and free shape agglomeration are pursued and achieved by 1 wt% AuNPs-organogel.

2. EXPERIMENTAL

The experiment was divided into three main stages. The first stage was focused on the synthesized of supramolecular organogel based on co-assembly of **BTAs** bearing hydrophobic (**1**) and amphiphilic (**2**) alkyl side chains. In addition, the second stage was synthesized AuNPs organogel using the organogel-template method via doping method. The last stage was the characterization of the physico-chemical properties of AuNPs organogel. In order to synthesize the BTAs organogel, compound 1 and 2 were first synthesized by Schotten Baumann reaction as shows in Scheme 1. Compound 1 and 2 were then mixed by molar ratio 1:1 in the presence of benzene as solvent. The mixture was allowed to evaporate at room temperature for 5-8 hours for gel formation. In the second stage, the resulting BTAs organogel was doped with 1 wt%, 3 wt%, and 5 wt% AuNPs separately. Later, in stage three, the resulting BTAs organogel and AuNPs-organogel were characterized to study their physico-chemical properties by using UV-Vis and Fluorescence spectroscopies, FT-IR, and TEM.

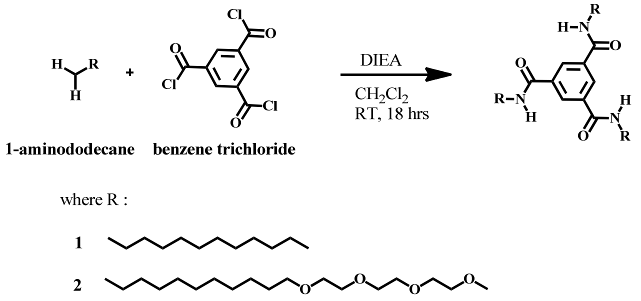

Scheme 1 Synthesis route of **BTA** bearing different side-chains

3. RESULTS AND DISCUSSION

3.1. Characterization of Hydrophobic BTA (1)

Characterization of **1** showed that the chemical shift of 1,3,5-benzene trichloride from 9.06 ppm was shifted to 8.31 ppm (singlet, 1H, d = Ar-H) indicating attachment of alkyl amide side chains to the carbonyl of benzene ring as in Figure 2(a). The ^{13}C-NMR spectrum in Figure 3(a) shows appearance of i at 167.22 ppm, which supported the bonding of amino to carbonyl. Nevertheless, the appearance of the peaks at 135.45 (j) and 127.12 (k) ppm indicates the presence of carbon for the benzene ring.

Characterization of **2** was carried out by using ^{1}H–NMR amd ^{13}C–NMR. In the case of ^{1}H–NMR spectrum as show in Figure 2(b), the chemical shift was observed from initial 2.85 ppm for 4 to 3.54 ppm due to methylene bonded to amide group. Chemical shifts at ^{13}C–NMR spectrum as show in Figure 3(b) was being observed to shifted from (a) 39.99 to 40.20 ppm with appearances of new peaks at (c) 126.43, (d) 132.21, (e) 136.24, and (f) 165.33 ppm.

(a)

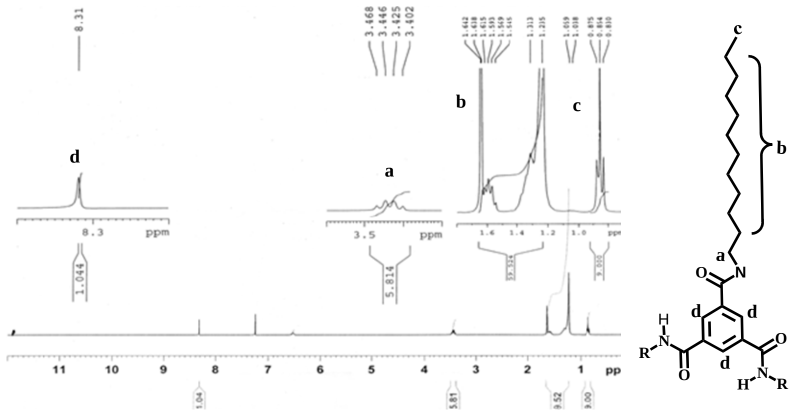

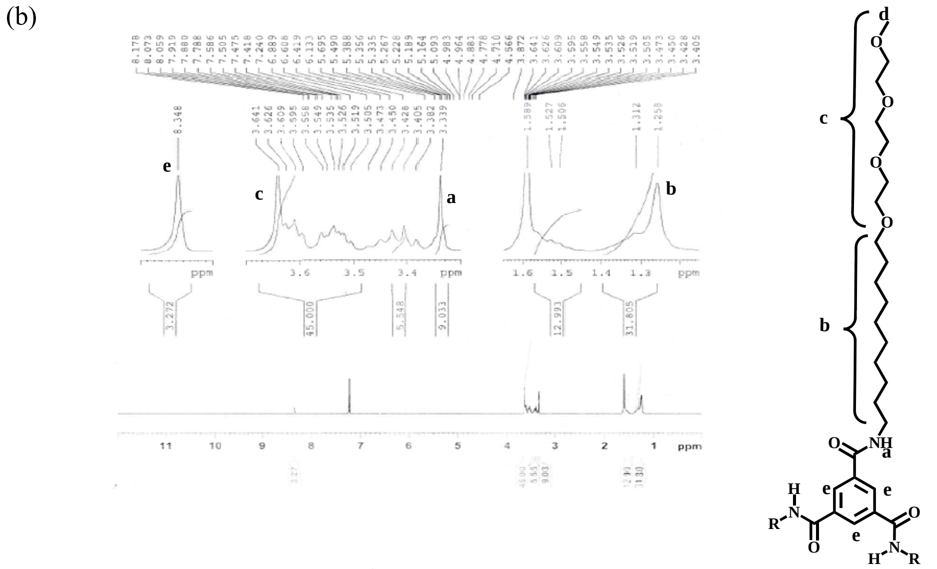

Figure 2 ^{1}H-NMR spectrum of (a) **1** and (b) **2**

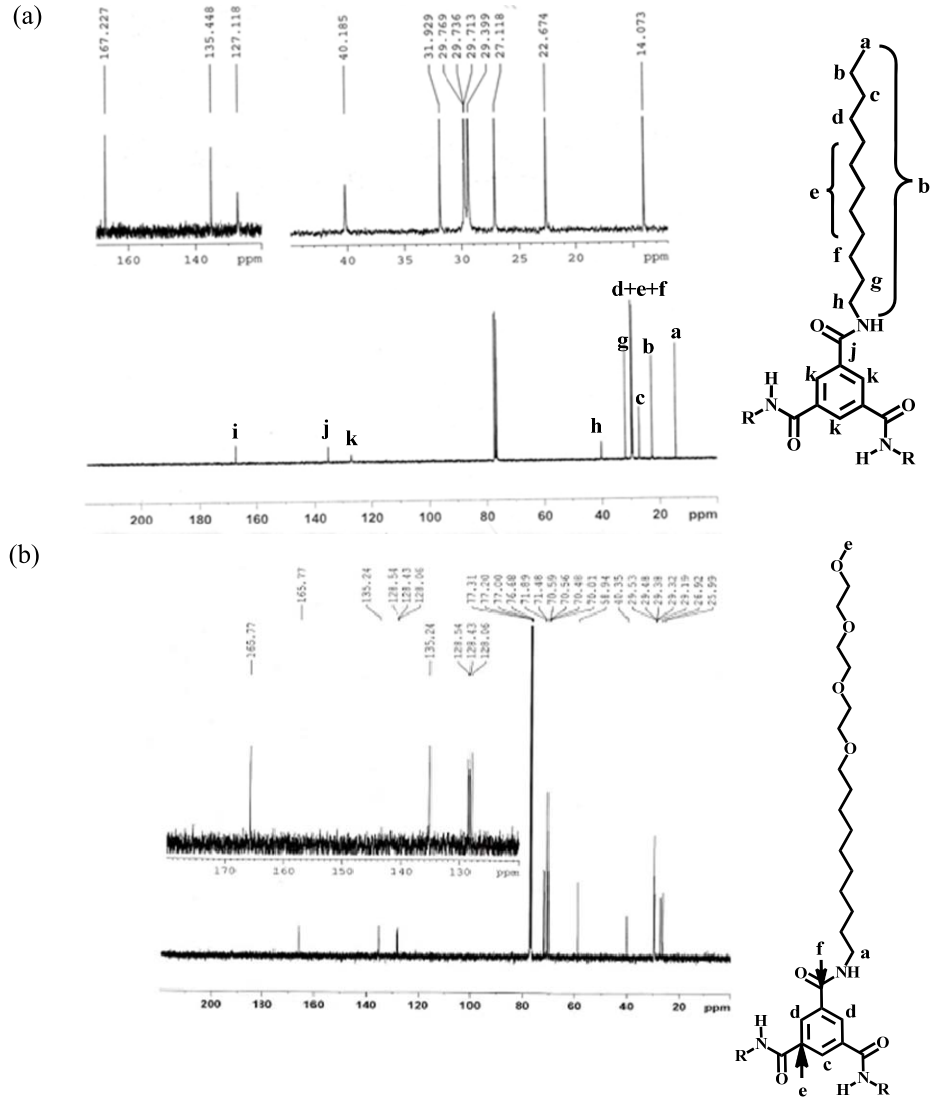

Figure 3 ^{13}C-NMR spectrum for (a) **1** and (b) **2**

3.2. Characterization of BTA_{1+2} Organogel by Co-Assembly Method

The gelling behaviours of **BTA_{1+2}** was studied using the inverted test flow method. Figure 4 shown the gelling behaviour of **BTA_{1+2}** organogel by inverted test flow in (a) while (b) **BTA_{1+2}** organogel observed under hand-held UV lamp 365 nm. The **BTA_{1+2}** organogel formed emitted an intense blue colour under a hand-held UV lamp with an

Figure 4 (a) Inverted test flow of **BTA_{1+2}** organogel and (b) **BTA_{1+2}** organogel observed under hand-held UV lamp 365 nm

3.3. Characterization of synthesized AuNPs-organogel using the organogel-template method via doping method

The fabrication of AuNPs source to **BTA_{1+2}** organogel for AuNPs-organogel was carried out in stage 2. The AuNPs source of various sizes 5 nm, 10 nm, 15 nm, and 20 nm were first diluted in benzene (100 mg) before being examined by using UV-Vis spectroscopy to study their SPR properties. The data obtained was shown as in Figure 5.

Based on Figure 5, UV-Vis spectra for all four sizes of AuNPs showed significant peaks at 530 nm indicated the presence of gold and due to its SPR property. The most intense peak was showed by (a) 5 nm AuNPs while the other sizes of AuNPs source gave lower intensity according to their size respectively. The (d) 20 nm AuNPs gave the lowest intensity due to its bigger size as compared to others. The highest absorption peak resulted from 5 nm AuNPs indicated its excellent SPR property. Hence, the 5 nm AuNPs source was chosen to be doped into **BTA_{1+2}** organogel to further study the physico-chemical properties of the AuNPs-organogel composite. The **BTA_{1+2}** organogel was doped with 5 nm AuNPs by 1 wt%, 3 wt% and 5 wt% to form AuNPs-organogel composites.

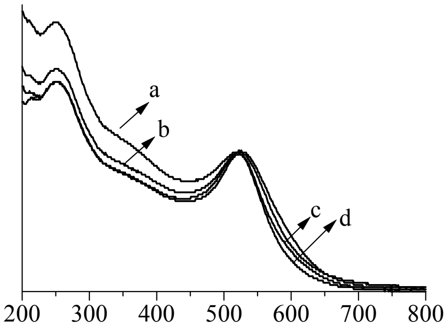

Figure 5 UV-Vis spectra of (a) 5 nm, (b) 10 nm, (c) 15 nm, and (d) 20 nm of AuNPs source diluted in benzene

3.4. Investigation the physico-chemical properties of AuNPs-organogel by utilizing the concentrations of AuNPs

The optical properties of the **BTA_{1+2}** organogel doped with varied wt% of 5 nm AuNPs were characterized by using 365 nm hand-held UV lamp. Based on the Figure 6, (i) showed all three samples of AuNPs-organogel while (ii) shows the comparison between original **BTA_{1+2}** organogel with varied wt % AuNPs-organogel. All samples gave blue colour emission under 365 nm hand-held UV lamp. Based on the observation, the original **BTA_{1+2}** organogel showed the the most intense blue colour emission as compared to others. As the wt% of AuNPs doped increased, the colour emission intensity of the **BTA_{1+2}** organogel was decreased respectively. This phenomenon was known as the quenching of the emission colour of the **BTA_{1+2}** organogel.

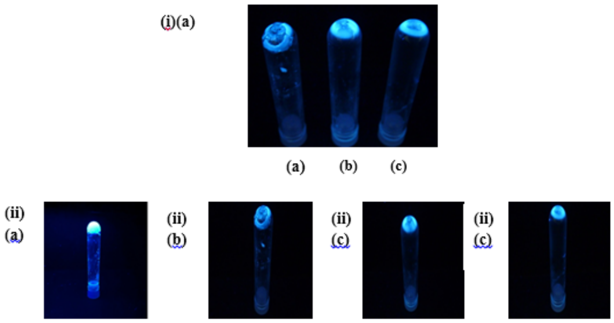

Figure 6 (i) (a) 1 wt%, (b) 3 wt%, and (c) 5 wt% of AuNPs doped to **BTA**$_{1+2}$ organogel and (ii) Comparison of SPR for (a) original **BTA**$_{1+2}$ organogel, (b) 1 wt%, (c) 3 wt%, and (d) 5 wt% of AuNPs doped to **BTA**$_{1+2}$ organogel observed under hand-held UV lamp 365 nm

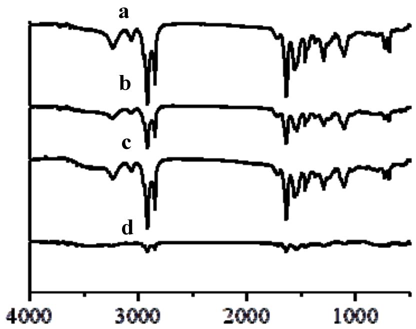

Figure 7 FT-IR spectra of (a) **BTA**$_{1+2}$ organogel, (b) 1 wt % of AuNPs-gel, and (c) 3 wt % (d) 5 wt % of AuNPs-organogel

FT-IR spectra above shown common vibration bands at 3233 and 1567 cm^{-1} due to formation of N−H bonding and vibration band at 1638 cm^{-1} due to formation of C=O bonding obtained from the **BTA**$_{1+2}$ organogel. In addition, FT-IR spectrum of (a), (b), (c), and (d) give three prominent vibrational peaks of 1620 and 1522 cm^{-1} due to formation of benzene ring and a vibration band at 1346 cm^{-1} due to formation of N=O bonding. Based on the FT-IR spectra in Figure 7, the transmittance % of (a) was the highest while (d) was the lowest. It is suggested that the decreasing of the transmittance % in (b), (c), and (d) is due to the composition of AuNPs in the organogel. Based on the spectra obtained, (b), (c), and (d) were quenching due to the presence of AuNPs in varied wt%. As the wt% of AuNPs to be doped to the organogel increased, the quenching pattern can be obviously observed at wavelength 2800 – 3500 nm.

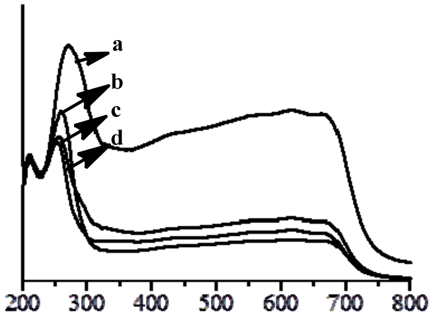

Figure 8 UV-Vis spectra of (a) original **BTA**$_{1+2}$ organogel, (b) 1 wt%, (c) 3 wt%, and (d) 5 wt% AuNPs-organogel respectively

There were three significant absorption bands that can be attributed for (a), (b), (c), and (d) at 210, 270, and broad shoulder from 400 to 850 nm. The intense bands at 210 nm were due to *π-π* stacking of benzene rings of the organogel. In addition, the absorption bands at 270 nm showed decreased in pattern proportional to the wt% AuNPs doped. This phenomenon indicated the quenching of the intensity ratio of the AuNPs-organogel. Particularly, absorption bands ranging from 400 to 850 nm at visible region indicates the electronic charge transfer occurring within the AuNPs-organogel composites. Based on Figure 8, the electronic charge transfer of (b), (c), and (d) were decreased as compared to (a). The decreasing of the electronic charge transfer of (b), (c), and (d) was due to the doping effect of AuNPs. It is suggested that the presence of AuNPs disturbed the electron transfer in the **BTA**$_{1+2}$ organogel networks system.

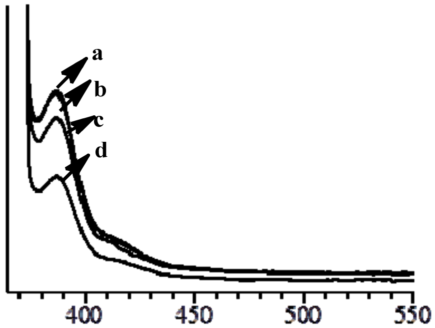

Figure 9 Emission spectra of (a) original $\mathbf{BTA_{1+2}}$ organogel, (b) 1 wt%, (c) 3 wt%, and (d) 5 wt% AuNPs-organogel

There was one significant emission spectra for all samples at wavelength between 480 – 490 nm. The emission spectra at this wavelength showed intensity decrement pattern. The highest intensity showed by (a) followed by (b), (c), and (d) respectively. The decrement pattern in intensity is probably due to the presence and composition of AuNPs. Based on Figure 9, spectrum (a) and (b) showed not much difference in intensity due to very small amount of AuNPs doped into the $\mathbf{BTA_{1+2}}$ organogel. Meanwhile, spectrum (c) and (d) showed significant decrease in intensity. This indicated the quenching of the intensity of the samples due to the composition of the AuNPs. As the wt% of AuNPs doped increased, the intensity of the emission spectra decreased.

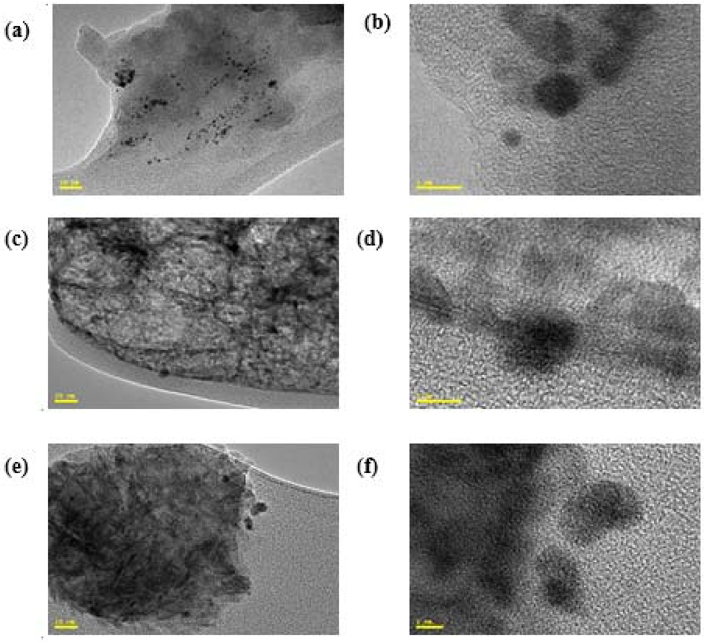

Figure 10 TEM images of (a) 1 wt%, (c) 3 wt%, and (e) 5 wt% AuNPs-organogel under 20 nm magnification while (b) 1 wt%, (d) 3 wt% and (f) 5 wt% AuNPs-organogel under 5 nm magnification

TEM images in Figure 10 showed the morphology and distribution of AuNPs-organogel for 1 wt%, 3 wt%, and 5 wt% under 5 and 20 nm magnification distinctively. Based on the images, (a) showed well-ordered arrangement of AuNPs in the $\mathbf{BTA_{1+2}}$ organogel template and free shape agglomeration. In the meanwhile, (c) and (e) showed bigger size of AuNPs cluster due to coagulation effect. This phenomenon indicated that the amount of AuNPs doped into the $\mathbf{BTA_{1+2}}$ organogel influenced the morphology, distribution and assembly of the AuNPs. Therefore, it is suggested that 1 wt% was the best wt% of AuNPs to be doped into that fixed weight of $\mathbf{BTA_{1+2}}$ organogel as it gave well-ordered arrangement and free shape agglomeration than others.

In addition, (b) was the magnified image of 1 wt% of AuNPs-organogel under 5nm magnification showed lattice structure of the AuNPs at facets (100) and (110). Interestingly, (d) also showed the lattice line on the $\mathbf{BTA_{1+2}}$ organogel structure. This indicated that the $\mathbf{BTA_{1+2}}$ organogel prepared was having crystalline structure property so called liquid crystal property. In (f), the image obtained showed bigger cluster AuNPs caused by coagulation effect due to high amount of AuNPs doped.

4. CONCLUSION

Hydrophobic BTA (**1**) was successfully prepared in 93% yield as a white powder solid through a single step Schotten-Baumann amidation reaction. Meanwhile, amphiphilic BTA (**2**) was successfully prepared in 38% yield as gel-like yellow oily liquid through 4 stepwise reactions via Schotten-Baumann reaction. The mixing of **1** and **2** resulted in the formation of organogel suitable for subsequent doping with 5 nm AuNPs. The BTAs organogel doped with 1 wt%, 3 wt%, and 5 wt% of 5 nm AuNPs. The physico-chemical properties of all AuNPs-organogels were characterized by FT-IR,TEM, UV-Vis, and Fluorescence spectroscopies. Based on TEM analysis, AuNPs-organogel with 1 wt% doped of AuNPs give well ordered and homogeneously distributed AuNPs-organogel morphology as compared with 3 wt% and 5 wt%. On the other hand, photophysical studies of AuNPs-organogel showed that as concentration of AuNPs increases, hypsochromic shift observed based on UV-Vis and quenching of emission intensity based on Fluorescence spectroscopies. The photophysical studies suggested that the increases loading of AuNPs strongly affected the molecular arrangements of co-assembled BTAs organogel. FT-IR spectra showed that there were quenching in the transmittance due to the presence of AuNPs in varied wt%. As the wt % of AuNPs to be doped to the organogel increased, the quenching pattern can be obviously observed at wavelength 2800 – 3500 nm.In conclusion, the set of characterization done onto the AuNPs-organogel showed that BTA organogel was a good template in synthesizing AuNPs with well-ordered arrangement and free shape agglomeration.

REFERENCES

[1] Lee, K. B., Lee, S. M., and Cheon, J. (2001). Size-Controlled Synthesis of Pd Nanowires Using a Mesoporous Silica Template via Chemical Vapour Infiltration. *Advanced Materials*. **13**, 517-520.

[2] Pissuwan, D., Niidome, T., and Cortie, M. B. (2011). The Forthcoming Applications of Gold Nanoparticles in Drug and Gene Delivery Systems. *Journal of Controlled Release.* **149(1)**, 65-71.

[3] El-Sayed, I. H., Huang, X., and El-Sayed, M. A. (2005). Surface Plasmon Resonance Scattering and Absorption of anti-EGFR Antibody Conjugated Gold Nanoparticles in Cancer Diagnostics: Application in Oral Cancer. *Nano Letters*. **5**, 829-834.

[4] Haruta, M.K., Sano, H., and Yamada,N. (1987). Novel Gold Catalysts for the Oxidation of Carbon Monoxide at a Temperature for Below 0 ^{0}C. *Chemistry Leters*. 405-408.

[5] Kasthuri, J., Veerapandian, S., and Rajendiran, N. (2009). Biological Synthesis of Silver and Gold Nanoparticles using apiin as Reducing Agent. *Colloids and Surfaces B: Biointerfaces*. *68*, 55-60.

[6] Jalani, M.A., Yuliati, L., and Lintang, H.O. (2013). Thermal Hydrogen Reduction for Synthesis of Gold Nanoparticles in the Nanochannels of Mesoporous Silica Composite. *Jurnal Teknologi*. **70**, 2180-3722.

[7] 7 Cantekin, S., Greef, T. F., and Palmans, A. R. (2012). Benzene-1,3,5-tricarboxamide: A Versatile Ordering Moiety for Supramolecular Chemistry. *Chemical Society Reviews*. **41**, 6125-6137.